Magnetic Resonance in Medicine

Reduction of motion effects in myocardial arterial spin labeling

Verónica Aramendía-Vidaurreta[1,2] iD | Pedro M. Gordaliza[3,4] iD | Marta Vidorreta[5] |
Rebeca Echeverría-Chasco[1,2] iD | Gorka Bastarrika[1,2] | Arrate Muñoz-Barrutia[3,4] iD |
María A. Fernández-Seara[1,2] iD

[1]Department of Radiology, Clínica Universidad de Navarra, Pamplona, Spain

[2]IdiSNA, Instituto de Investigación Sanitaria de Navarra, Pamplona, Spain

[3]Department of Bioengineering and Aerospace Engineering, Universidad Carlos III de Madrid, Madrid, Spain

[4]Instituto de Investigación Sanitaria Gregorio Marañón, Madrid, Spain

[5]Siemens Healthineers, Madrid, Spain

Correspondence
María A. Fernández-Seara, Department of Radiology, Clínica Universidad de Navarra, Pio XII, 36, 31008 Pamplona, Spain.
Email: mfseara@unav.es

Purpose: To evaluate the accuracy and reproducibility of myocardial blood flow measurements obtained under different breathing strategies and motion correction techniques with arterial spin labeling.

Methods: A prospective cardiac arterial spin labeling study was performed in 12 volunteers at 3 Tesla. Perfusion images were acquired twice under breath-hold, synchronized-breathing, and free-breathing. Motion detection based on the temporal intensity variation of a myocardial voxel, as well as image registration based on pairwise and groupwise approaches, were applied and evaluated in synthetic and in vivo data. A region of interest was drawn over the mean perfusion-weighted image for quantification. Original breath-hold datasets, analyzed with individual regions of interest for each perfusion-weighted image, were considered as reference values.

Results: Perfusion measurements in the reference breath-hold datasets were in line with those reported in literature. In original datasets, prior to motion correction, myocardial blood flow quantification was significantly overestimated due to contamination of the myocardial perfusion with the high intensity signal of blood pool. These effects were minimized with motion detection or registration. Synthetic data showed that accuracy of the perfusion measurements was higher with the use of registration, in particular after the pairwise approach, which probed to be more robust to motion.

Conclusion: Satisfactory results were obtained for the free-breathing strategy after pairwise registration, with higher accuracy and robustness (in synthetic datasets) and higher intrasession reproducibility together with lower myocardial

blood flow variability across subjects (in in vivo datasets). Breath-hold and synchronized-breathing after motion correction provided similar results, but these breathing strategies can be difficult to perform by patients.

1 | INTRODUCTION

Reduced myocardial perfusion reserve, computed as the ratio of stress to rest myocardial blood flow (MBF), is an indicator of ischemia and is associated with obstructive coronary artery disease, which to date is the most prevalent cardiovascular disease with high morbidity and mortality.[1,2] In MRI, perfusion can be clinically evaluated with first-pass imaging but requires the injection of a Gadolinium-based contrast agent. Alternatively, arterial spin labeling (ASL) can measure MBF noninvasively by magnetically labeling water protons contained in arterial blood,[3,4] facilitating perfusion measurements in a wider scope of patients, such as those with renal dysfunction or with an allergy to contrast agents. Most previous research in cardiac ASL has used flow-sensitive alternating inversion recovery (FAIR) labeling, which alternates selective and nonselective radiofrequency inversion pulses for control and label acquisitions, respectively.

The application of cardiac ASL is challenging due to the presence of motion that appears as a result of heart rate variations, breathing patterns, and other involuntary movements during the MRI study. The perfusion-weighted signal is obtained after subtraction of label from control images; thus, it is sensitive to motion not only across the temporal series but also between image pairs. In addition, ASL is a low SNR technique and requires temporal averaging of the perfusion-weighted images (PWIs). Although averaging allows to improve image quality and reduce noise, it can also introduce blurring artifacts if motion is not correctly minimized. Motion during the cardiac cycle has been typically tackled with the use of prospective electrocardiogram gating. In myocardial ASL, 2 approaches have been used: single[5–8] and double[9,10] gating.

The natural breathing pattern at rest, also called tidal breathing, causes motion of the heart mainly through the diaphragm and chest wall displacements. The respiratory rate in healthy adults typically varies between 12 and 24 breaths per min (2.4 to 5 s duration).[11] The highest degree of motion occurs in the superoinferior direction with a displacement of around 18.1 ± 9.1 mm.[12]

Through-plane motion can be especially problematic in FAIR ASL acquisitions because it can degrade the slice-selective inversion efficiency, leading to signal from static tissue not being properly inverted and contributing to an overestimation of perfusion. This is commonly prevented with the use of an increased slice-selective volume containing the image plane and 2 gaps of equal size above and below it, which assures that the image slice is inverted despite the presence of a certain degree of motion. Nevertheless, there is a need to reduce subtraction errors due to motion effects during the image readout, and thus avoid the position mismatch of the myocardium in label and control acquisitions.

Strategies to reduce motion due to respiration include breath-hold,[5–8,13] synchronized-breathing,[9,14] navigator-gating,[15] or free-breathing,[16] followed by nonrigid registration approaches. Breath-hold strategies minimize respiratory motion but introduce a time limitation for the acquisition of perfusion images, which is typically restricted to 1 ASL pair in a 12-heartbeat breath-hold duration. Longer durations might be challenging to apply in the clinical practice, especially under stress conditions. This requires the use of consecutive breath-holds, separated by normal breathing periods. However, multiple breath-holds are not necessarily equally performed, which could result in the acquisition of images at different expiratory positions. This hinders a direct voxel-wise subtraction and averaging of the PWIs. Navigator-gating strategies serve to synchronize the end-expiratory phase of the respiration with imaging. However, a low navigator acceptance rate can lead to extremely long scan times.

Synchronized breathing has been successfully employed in abdominal MRI imaging, particularly in renal ASL to minimize respiratory motion.[17] However, this strategy is less extended in cardiac ASL, where only 2 studies have tested its use.[9,14] Synchronized breathing requires the subject's cooperation to perform a short breath-hold during the timing of inversion and readout, whereas normal breathing is allowed in the remaining time of the sequence. Therefore, this technique is expected to minimize the degree of motion caused during tidal breathing similarly to breath-holding while increasing the time efficiency of the repeated acquisitions.

However, in patient populations with difficulty in holding their breath, free-breathing acquisitions

are often preferred. These need to be combined with registration, although the effects of through-plane motion in 2D acquisitions cannot be entirely corrected. Registration approaches can be divided based on their complexity into rigid (Euclidean transformations) and nonrigid (affine and projective transformations). For cardiac applications, it has been shown that rigid registrations cannot entirely compensate for the tissue deformations of the heart[18]; thus, nonrigid approaches are typically used. The registration of a stack of images, such as the those acquired with ASL, can be performed using 2 different approaches, named pairwise or groupwise, according to the way the temporal images are aligned to each other.

The pairwise approach requires the selection of a reference image to which the other images are registered. Motion in cardiac ASL has been typically minimized in this manner, with label and control images being independently registered to their correspondent reference due to their intensity contrast differences[16,19] or by further alignment of the PWIs to a reference.[15] Commonly used similarity metrics to evaluate registration performance include mutual information robust against global intensity changes and correlation-based metrics robust to local inhomogeneities.[20]

The groupwise approach, successfully employed in other quantitative cardiac MRI techniques such as T_1 mapping,[21] performs a simultaneous registration to align the multiple images to a mean space. It has the advantage of incorporating temporal information into the registration procedure while reducing the bias introduced by the choice of a reference image in the pairwise method. Commonly used similarity metrics, such as principal component analysis (PCA), are based on the intensity variance reduction along the stack of images. PCA relies on the fact that the intensity at each voxel of the image through time can be described by a low dimensional signal model without having prior knowledge of the specific model.[21] For this reason, in the context of myocardial ASL, the groupwise method is expected to differentiate between the trajectories of alternating intensity changes of the blood pool (low intensity in label images and high intensity in control images) and the presence of motion, while allowing a simultaneous registration of the baseline, label, and control acquisitions.

The objectives of this study were to investigate the use of different breathing strategies, named breath-hold, synchronized-breathing, and free-breathing, combined with motion detection or registration algorithms (evaluating pairwise and groupwise approaches in synthetic and in vivo datasets), and to assess their effects on the accuracy and reproducibility of myocardial perfusion measurements.

2 | METHODS

Twelve healthy volunteers (age (mean ± SD) 29 ± 3 years; 6 females) underwent a cardiac MRI study on a 3 Tesla system (Magnetom Skyra, Siemens, Erlangen, Germany), equipped with a 32-channel spine and an 18-channel body array coil. The study was approved by the Ethics Committee of the University of Navarra. Written informed consent was obtained from all participants.

2.1 | ASL sequence

A FAIR ASL sequence was employed to image a midventricular short-axis slice. The sequence comprised 4 presaturation pulses followed by a hyperbolic secant adiabatic inversion pulse alternated between nonselective and slice-selective, a TI of 1 s, and a single-shot balanced steady-state free precession (bSSFP) readout with fat saturation. The nonselective inversion slab thickness was 390 mm, and the slice-selective inversion slab thickness was 30 mm to minimize the effects of motion.

Imaging parameters were: matrix size = 128 × 104, FOV = 300 × 243 mm^2, isotropic pixel-size = 2.34 × 2.34 mm^2, slice thickness = 10 mm, flip angle = 70°, GRAPPA-2-integrated (24 reference lines), TE = 1.23 ms, TR_{bSSFP} = 2.39 ms, readout duration = 150 ms, and bandwidth = 908 Hz/pixel.

The sequence used single electrocardiogram gating. Ideally, both the inversion pulse and image readout should take place during mid-diastole. This was attempted with the use of a specific time delay, adjusted once at the beginning of each dataset and kept constant for all control and label pairs within the sequence. Adjustment was performed for every subject according to its RR interval, defined as the time between 2 consecutive R waves of the electrocardiogram, to deal with the possible heart rate variations that might occur during the scanning session. The TI remained fixed to 1 s regardless of the time delay.

2.2 | MRI protocol

The imaging protocol consisted in acquiring ASL images under 3 breathing strategies, as shown in Figure 1:

1. Breath-hold (BH): Subjects were given instructions to perform 6 consecutive breath-holds. Each breath-hold had an approximate duration of 12 s and comprised the acquisition of 1 pair of label and control images. This resulted in the acquisition of a total of 12 images within 2 min of scan time. The minimum TR of the sequence was set to 6 s.
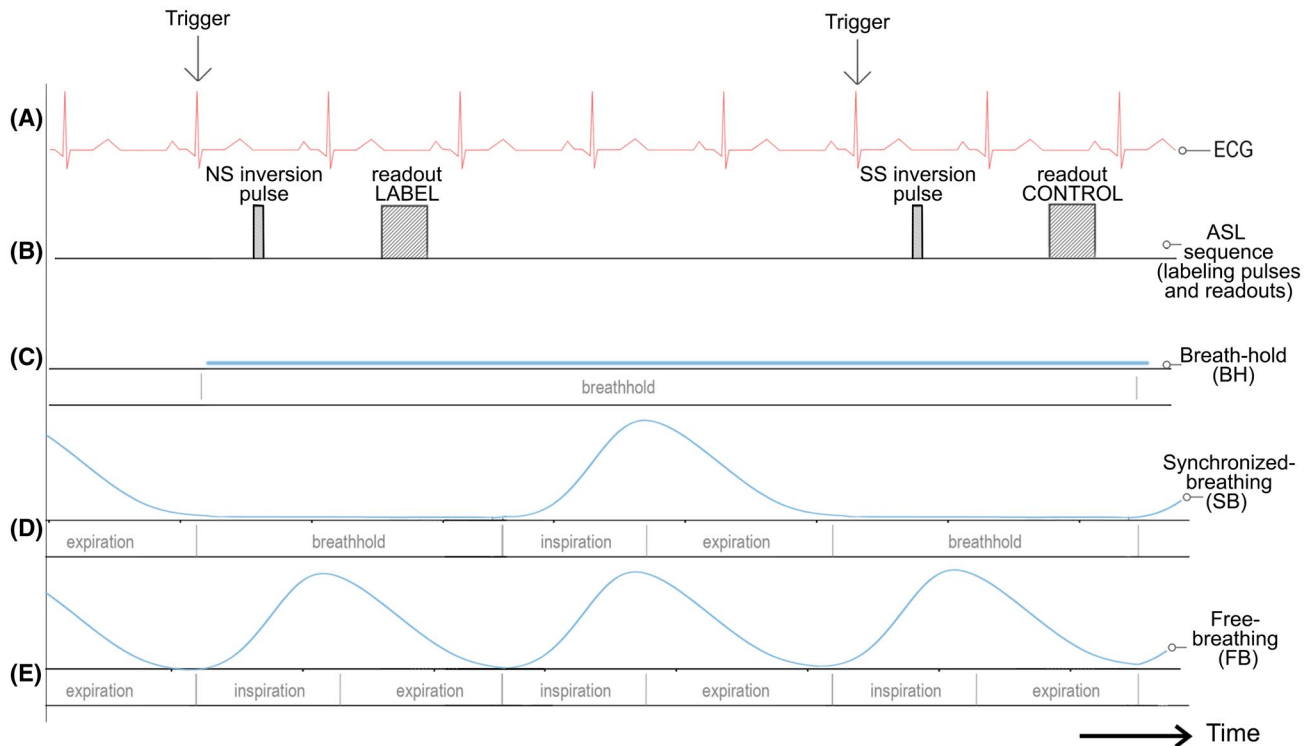
FIGURE 1 Breathing strategies employed during the acquisition of ASL images. (A) ECG gating employed during the ASL sequence acquisition. (B) Timing of labeling pulses and readouts for a pair of label and control acquisitions. Three breathing strategies were used: (C) breath-hold: short breath-holds were performed during the acquisition of each label and control image pair; (D) synchronized-breathing: subjects were trained to synchronize their respiration with the TR of the sequence; and (E) free-breathing: subjects were asked to breathe normally. ASL, arterial spin labeling; ECG, electrocardiogram; NS, nonselective; SS, slice-selective

2. Synchronized-breathing (SB): Subjects were trained outside and inside the scanner to recognize the readout sound and to synchronize their respiration to the TR of the sequence, which was set to a minimum of 5 s. The synchronized respiration included 2 periods that started after the first readout sound and were repeated until the entire dataset was acquired. These consisted in performing a short inspiration and expiration (of about 2 to 3 s), followed by a short breath-holding at the time of exhalation until the next readout sound. In this manner, the breath-hold duration included both inversion pulse and image acquisition. A total of 62 images were acquired in an approximate scan time of 5 min.
3. Free-breathing (FB): Subjects were asked to breathe normally. A total of 62 images were acquired in an approximate scan time of 5 min. The minimum TR was set to 5 s.

Motion was expected to be minimized in BH and SB strategies in which, unlike FB, there is an effort to freeze respiratory motion. Two ASL datasets were acquired with each breathing strategy to assess intrasession reproducibility. The breathing strategy order was alternated among volunteers to avoid any possible order effect in the study. A baseline image (without presaturation and inversion pulses) was independently acquired within a breath-hold for each dataset.

2.3 | Postprocessing

Perfusion images acquired in all breathing strategies were analyzed, without any motion correction step, after detecting and discarding motion outliers, as well as after groupwise and pairwise registrations.

2.3.1 | Motion detection

The respiratory phase at which the images were acquired can be identified based on the position of the diaphragm. During inspiration, the diaphragm contracts and descends; whereas during expiration, the diaphragm relaxes and moves up.

To evaluate the amount of respiratory motion in the original perfusion datasets, a voxel within the anterior myocardial segment was manually selected in an image acquired at expiration (see Supporting Information Figure S1). The presence of motion along the superoinferior direction could be detected by an intensity change at this

voxel, which varied between the intensity of the myocardium and the lungs.

To quantify the degree of motion, the mean and SD of this voxel's intensity across images were recorded. Outliers were identified as those images whose intensity at this voxel was below the mean minus 1 SD. When an outlier was detected (either a label or a control image), the corresponding PWI was discarded.

2.3.2 | Image registration

Registration was applied to the original perfusion datasets using both pairwise and groupwise approaches implemented in Elastix (Binaries 4.9.0).[22] Registration parameters are specified in Table 1. Groupwise parameters were adapted from those used in Huizinga et al.[21,23] for the registration of T_1-MOLLI images of the heart. Pairwise parameters were chosen as similar as possible. Their performance was evaluated in synthetic and in vivo ASL datasets. In vivo datasets were masked around the heart prior to registration with a circular region of interest (ROI) to reduce the influence of the surrounding organs but large enough to contain the heart despite the presence of motion.

Pairwise
The reference label-control image pair was automatically selected as the highest correlated label-control pair (see Supporting Information Figure S3). Then, the reference control was registered to the reference label image. Subsequently, label and control images were independently registered to their corresponding reference. In total, 62 different pairwise registrations were performed; 31 labels were aligned with the reference label; and 31 controls were aligned with the registered reference control.

Groupwise
To compute PCA metric, temporal ASL images can be incorporated as columns in a matrix from where the correlation matrix (K) is calculated.[21] PCA is calculated on K to obtain the corresponding eigenvalues, which represent the explained variance along the principal components. A dissimilarity metric (D_{PCA}) is defined as follows[21]:

$$D_{PCA}(\mu) = N - \sum_{j=1}^{L} \lambda_j(\mu),$$

where j is the rank of eigenvalues; λ_j is the jth eigenvalue of K; μ is a set of transformation parameters; N is the total number of images; and L is a user-defined parameter ($1 < L < N$). By minimizing a cost function based on D_{PCA}, images are transformed by a set of parameters so that the eigenvalue spectrum of K approaches the spectrum of an aligned set of images.

Evaluation in synthetic ASL images
Synthetic images were created from FB in vivo datasets in a random subgroup of 8 subjects by manually segmenting and assigning specific intensities to the following ROIs: blood (255 in control and 42 in label images), left ventricular myocardium (85), and background (0). Subsequently, images were corrupted with Gaussian noise (0 mean and 1.30 SD) to achieve similar SNR to that of in vivo images and smoothed with a Gaussian filter (kernel size = 3 × 3 and sigma levels = 0.4 and 0.45) to simulate the effects of partial volume. The parameters of the Gaussian filter were selected based on the intensity profile of the interface between myocardium and lungs in in vivo images. Reference perfusion signal values in the myocardium were obtained from the set of smoothed synthetic images applying the

TABLE 1 Parameters used in the groupwise and pairwise nonrigid registrations of myocardial ASL images

	Parameters
Groupwise	All images: • Principal component analysis metric (number of eigenvalues = 3) • B-spline stack transform with a final grid spacing of 32
Pairwise	Reference images: • Mutual information metric • B-spline transform with a final grid spacing of 32 All images: • Normalized correlation metric • B-spline transform with a final grid spacing of 32
Common	• 2 resolutions with a downsampling factor of 2 and 1 for *x-y* dimensions • 1000 iterations were set for the adaptive stochastic gradient

In the pairwise registration approach, parameters listed under "reference images" were used in the registration of the reference control to the reference label image, whereas parameters listed under "all images" were employed in the registration of first, the entire set of label images to the reference label, and then the entire set of control images to the registered reference control.

Abbreviation: ASL, arterial spin labeling.

manual myocardial segmentations. These values were considered ground truth.

In addition, to assess the amount of motion that the registration algorithms can correct, a series of affine transformations were applied to a synthetic label and control image (smoothed with sigma = 0.4 and corrupted with noise). Five datasets of 62 images were generated for each transformation, increasing the amplitude of the motion. The amount of motion within a dataset was randomly selected. As represented in Supporting Information Figure S2, transformations were: horizontal and vertical translation (displacement was varied between 1 to 5 pixels), rotation (angle was varied between 5° to 25°), and horizontal shear (angle was varied between 5° to 25°).

All synthetic datasets, with natural and introduced motion, were analyzed before and after registration. After subtraction of label from control images, a manual ROI was delineated in the myocardium over the mean PWI. The registration performance was evaluated by comparison of mean perfusion signal and the percentage of accuracy error, computed as the absolute difference between measured and reference perfusion signal divided by the reference and multiplied by 100 on the mean PWI.

2.3.3 | In vivo data analysis

Control and label images were pairwise subtracted and averaged. A myocardial ROI was manually drawn in the average PWI (in all datasets) and baseline image (in all datasets except those analyzed after groupwise registration). Outliers in the temporal ASL series were excluded if deviated from the mean by more than 2 SD.

BH datasets were also postprocessed, as it has been performed typically in literature, by manually drawing a myocardial ROI for each PWI. In this manner, the effects of motion between breath-holds were minimized. These measurements were considered as the reference perfusion in in vivo images.

MBF was quantified following the equation:

$$\text{MBF (mL/g/min)} = \frac{\lambda \cdot \Delta M}{2 \cdot M0 \cdot TI \cdot e^{-TI/T1}} \cdot 60,$$

where ΔM is the mean myocardial perfusion-weighted signal; M_0 is the myocardial signal from the baseline image; TI is the inversion time (1000 ms); and T_1 is the T_1 of arterial blood (1664 ms at 3 Tesla[24]).

From the MBF time series for each subject, physiological noise (PN) was evaluated by computing the MBF SD divided by the square root of the number of averages.[5]

MBF variability across subjects was evaluated by calculating the coefficient of variation across subjects (CV_{MBF}) as the ratio of the MBF group SD to the group mean.

The minimum number of PWIs required in SB or FB datasets after pairwise registration to match the PN performance of the reference BH measurements was investigated by evaluating perfusion as a function of the number of averages considering data obtained in the first acquisition.

2.4 | Statistical analysis

A significance level of 0.05 was used for all analyses.

For synthetic data representing natural FB motion, a Friedman test was used to evaluate perfusion differences across groups (reference, with and without registration). Post hoc comparisons were performed with the Wilcoxon signed-rank test adjusting P values with the Bonferroni correction.

For in vivo data obtained from the first acquisition, 2 nonparametric factorial analysis of variances[25] for repeated measurements were performed to evaluate differences in MBF and PN across 2 factors: breathing strategy (3 levels = BH, SB, and FB) and motion-correction technique (4 levels = without any motion correction step, after groupwise registration, after pairwise registration, and after detecting and discarding motion outliers). Post hoc comparisons were performed with the Wilcoxon-signed rank test adjusting P values with the Bonferroni correction. Wilcoxon signed-rank tests were also used to compare MBF and PN obtained in all datasets with the reference BH measurements.

Taking into account data from the 2 acquisitions, intrasession reproducibility was assessed through the within-subject coefficient of variation (wsCV), as[26,27]:

$$\text{wsSD} = \sqrt{\frac{\sum_{s=1}^{n} \left(x_1 - x_2\right)^2}{2n}}$$

$$\text{Mean} = \frac{\sum_{s=1}^{n} \left(x_1 + x_2\right)}{2n}$$

$$\text{wsCV}(\%) = \frac{\text{wsSD}}{\text{Mean}} \cdot 100,$$

where n is the number of subjects, and x_1 and x_2 are the duplicate perfusion measurements for each subject. Finally, Bland-Altman plots were computed to assess the agreement between measurements.

3 | RESULTS

3.1 | Evaluation of motion detection

The number of discarded and remaining PWIs is reported per subject in Supporting Information Table S1. On average, the number of discarded PWIs in the first acquisition of the BH, SB, and FB datasets was 1 ± 1, 8 ± 3, and 10 ± 4, respectively.

3.2 | Evaluation of synthetic image registration

Panel A of Figure 2 shows the motion evaluation of synthetic datasets representing natural FB motion with the obtained perfusion boxplots across registration techniques. The Friedman test revealed significant differences in perfusion signal ($P_{sigma = 0.4} = 0.0009$, $P_{sigma = 0.45} = 0.001$) and accuracy errors ($P_{sigma = 0.4} = 0.001$, $P_{sigma = 0.45} = 0.03$). Post hoc comparisons showed that these differences lied between datasets without registration and all others ($P = 0.04$ for all comparisons), whereas no differences were found between datasets after registration and the reference measurements. Table 2 shows perfusion signal and accuracy errors obtained across subjects. Accuracy errors were significantly decreased with the use of both registration approaches ($P_{sigma = 0.4} = 0.01$, $P_{sigma = 0.45} = 0.04$). They were lower after pairwise than groupwise registration, although differences were not significant. Accuracy error was increased in datasets with lower perfusion. The sigma level of 0.4 provided a perfusion signal between 6% to 8%, which is closer to previously reported signal in myocardial ASL (between 1% to 8%).[28]

Panel B of Figure 2 shows the motion evaluation of synthetic images corrupted with different degrees of motion. It can be observed that the overestimation of the perfusion signal was increased with the motion amplitude and reduced after registration. Overall, pairwise registration presented a much lower accuracy error than the groupwise approach, regardless of the transformation offering a robust performance for all amplitudes.

3.3 | Qualitative evaluation of in vivo image registration

Figure 3 shows an original BH, SB, and FB dataset and a registered FB dataset from a representative subject. The SD across PWIs of the BH dataset is high due to the effects of motion between breath-holds. The same occurs with the original FB dataset due to the presence of motion between images. This is successfully reduced after registration. Results obtained with both registration approaches are visually comparable.

3.4 | In vivo quantification

Panel A of Figure 4 shows the MBF boxplots across breathing strategies and motion correction techniques. Perfusion is overestimated in original datasets due to the particularly high intensity signal of blood pool present in the PWIs. This overestimation was corrected with the use of motion correction techniques, obtaining quantitative perfusion values consistent with those presented in PET literature.[29] The factorial analysis of variance revealed a significant interaction ($P = 0.00013$). Post hoc tests P values are indicated in Table 3. Comparisons with reference BH measurements showed significant perfusion differences with the original SB and FB datasets ($P = 0.04$ and $P = 0.03$ for SB and FB datasets, respectively) and with the SB dataset after motion detection ($P = 0.03$).

Panel B of Figure 4 shows the PN boxplots. The factorial analysis of variance revealed no significant interaction ($P = 0.36$). Post hoc tests P values are indicated in Table 3. Comparisons with the reference BH measurements showed no significant differences.

The quantitative values presented in Table 4 confirm that MBF variability across subjects was higher in original datasets. This was reduced after motion correction, and in particular after pairwise registration, as can be observed in the computed CV_{MBF}. Another interesting aspect is that the first original SB dataset presents higher variability across subjects than the second one, which could be related to the fact that repetition helped in the performance of the synchronization.

In SB and FB datasets after pairwise registration, PN decreased with the number of averaged PWIs, as expected. Figure 5 shows that the number required to match the PN performance of the reference BH dataset was 8 for SB and 15 for FB. Very little PN decrease was observed after 20 averages in the SB dataset and after 25 averages in the FB dataset.

3.5 | Reproducibility

Table 4 also shows the wsCV obtained across subjects for each dataset. BH with individual ROIs, SB after pairwise registration, and FB after pairwise registration showed the best reproducibility results with a wsCV of 16%, 17%, and 11%, respectively.

Figure 6 shows the Bland-Altman plots of MBF measurements for all datasets. A lack of agreement can be observed in original datasets, whereas measurements after motion correction present narrower limits of agreement, indicating more confident measurements.
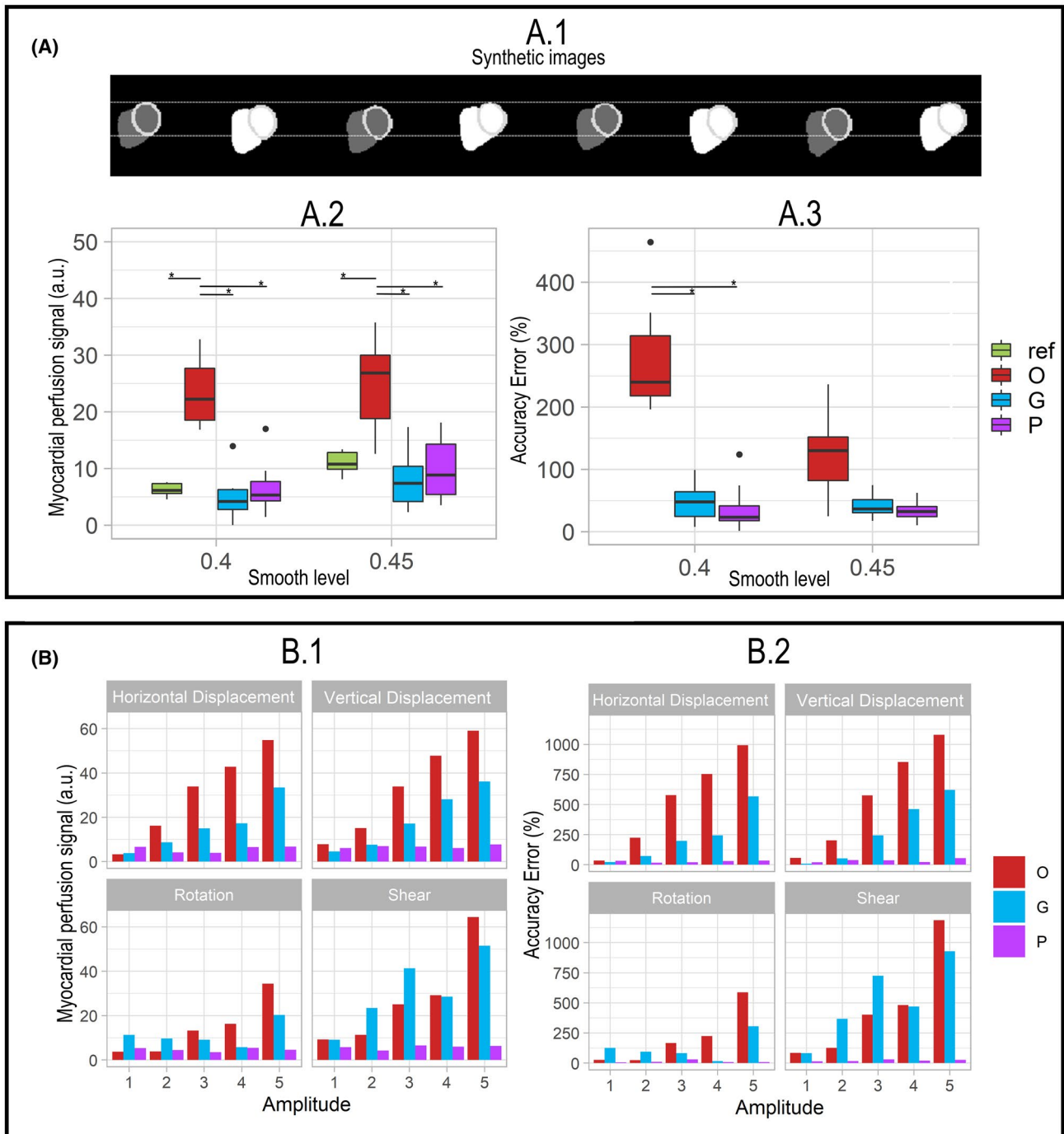
FIGURE 2 Motion evaluation in synthetic images. Panel A: synthetic images with natural motion (A.1). A subset of synthetic ASL images created from the segmentation of in vivo FB datasets from a representative volunteer. Slashed horizontal lines are depicted at the edges of the myocardium to better show movement across images. Boxplots for: (A.2) myocardial perfusion signal (a.u), and (A.3) accuracy error (%) obtained from the mean perfusion-weighted image (*indicates significant differences between datasets). Panel B: synthetic images with introduced motion. Bar graphs for: (B.1) myocardial perfusion signal (a.u), (B.2) accuracy error obtained from the mean perfusion-weighted image for different motion amplitudes. For data without motion correction (in red), data after groupwise registration (in blue), data after pairwise registration (in pink), and ref data (in green). FB, free-breathing; G, data after groupwise registration; O, data without motion correction; P, data after pairwise registration; ref, reference

4 | DISCUSSION

In this study, ASL images were acquired using different breathing techniques named BH, SB, and FB. Prior to the

perfusion data analysis, 2 motion correction methods were evaluated: detection and discarding of motion outliers and image registration. Motion detection was performed based on the temporal intensity variation of a voxel located in

TABLE 2 Myocardial perfusion measurements and accuracy errors obtained from synthetic datasets across subjects

		Gaussian Smoothing Level	
		0.40	**0.45**
Myocardial perfusion signal (a.u.)	Original	22.26 (18.33-29.46)	26.87 (16.1-31.14)
	Groupwise registration	4.20 (2.23-6.43)	7.40 (4.1-11.37)
	Pairwise registration	5.34 (3.84-8.96)	8.87 (4.33-14.48)
	Reference intensity	6.16 (5.34-7.48)	10.79 (9.44-13.06)
	Reference perfusion (%)	6.95 (6.06-8.35)	11.80 (10.42-14.04)
Accuracy error (%)	Original	239.93 (207.51-338.85)	130.14 (67.4-171.76)
	Groupwise registration	48.18 (17.69-78)	36.71 (27.61-59.14)
	Pairwise registration	23.50 (14.17-63.37)	32.42 (23.46-50.99)

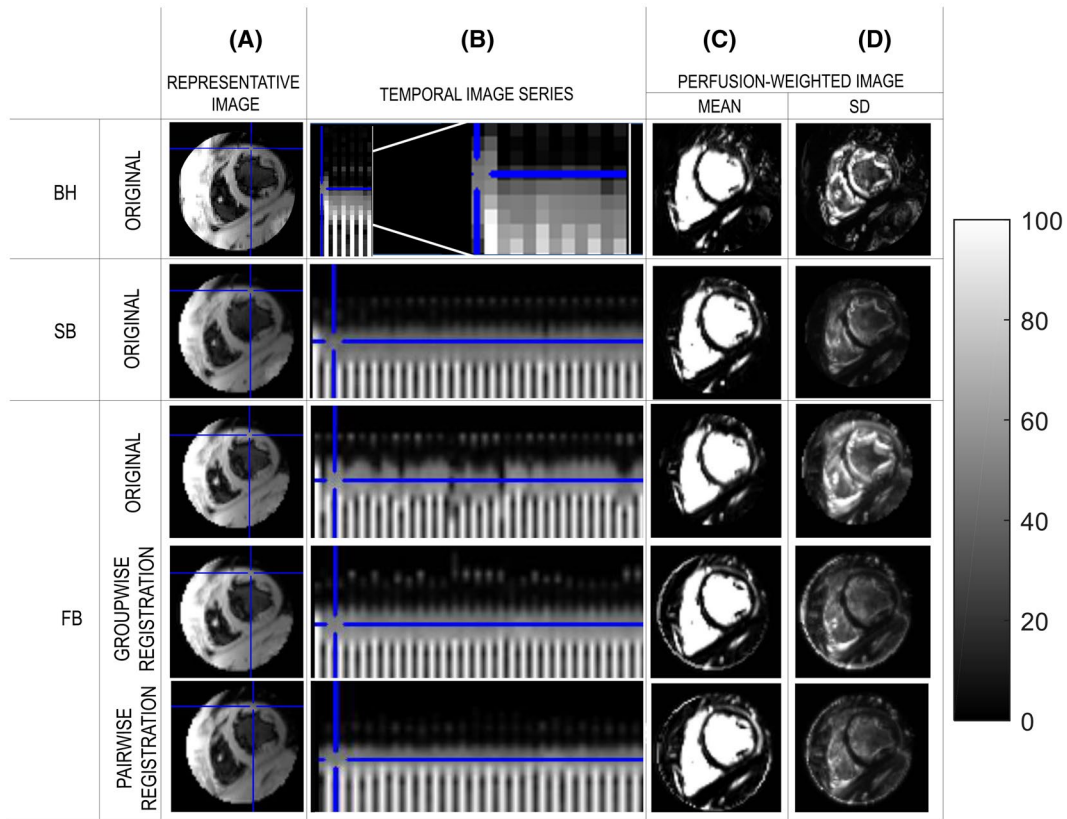All values are shown as median (interquartile range).

FIGURE 3 Motion effects from a representative volunteer. From top to bottom: BH, SB, and FB datasets. FB datasets are presented with and without image registration, considering groupwise and pairwise approaches. For each in vivo perfusion dataset, the panels show: (A) representative label image with a cross-mark in the anterior myocardial voxel, and (B) intensity of the selected voxel across the temporal image series. For BH, the temporal series has been zoomed to better see intensity differences across images. (C) Mean perfusion-weighted image. (D) SD of the perfusion-weighted images. Original datasets, representing data without motion correction, have also been masked for better image comparison. BH, breath-hold; FB, free-breathing; SB, synchronized-breathing

the anterior myocardial segment. Registration was carried out using groupwise and pairwise nonrigid approaches, whose performance was compared in synthetic data by computing the accuracy error obtained after registration, and in vivo data based on the perfusion variability across subjects and intrasession reproducibility. Synthetic data was also used to evaluate the robustness of the registration to increasing degrees of motion. The groupwise

registration of in vivo myocardial ASL images was feasible, allowing the simultaneous alignment of baseline, label, and control images. Pairwise registration was also feasible, and the bias introduced by the choice of a reference image was minimized with the automatic selection of the highest correlated label-control pair.

The BH strategy was guided by auditory instructions. Its performance was dependent on the success of the
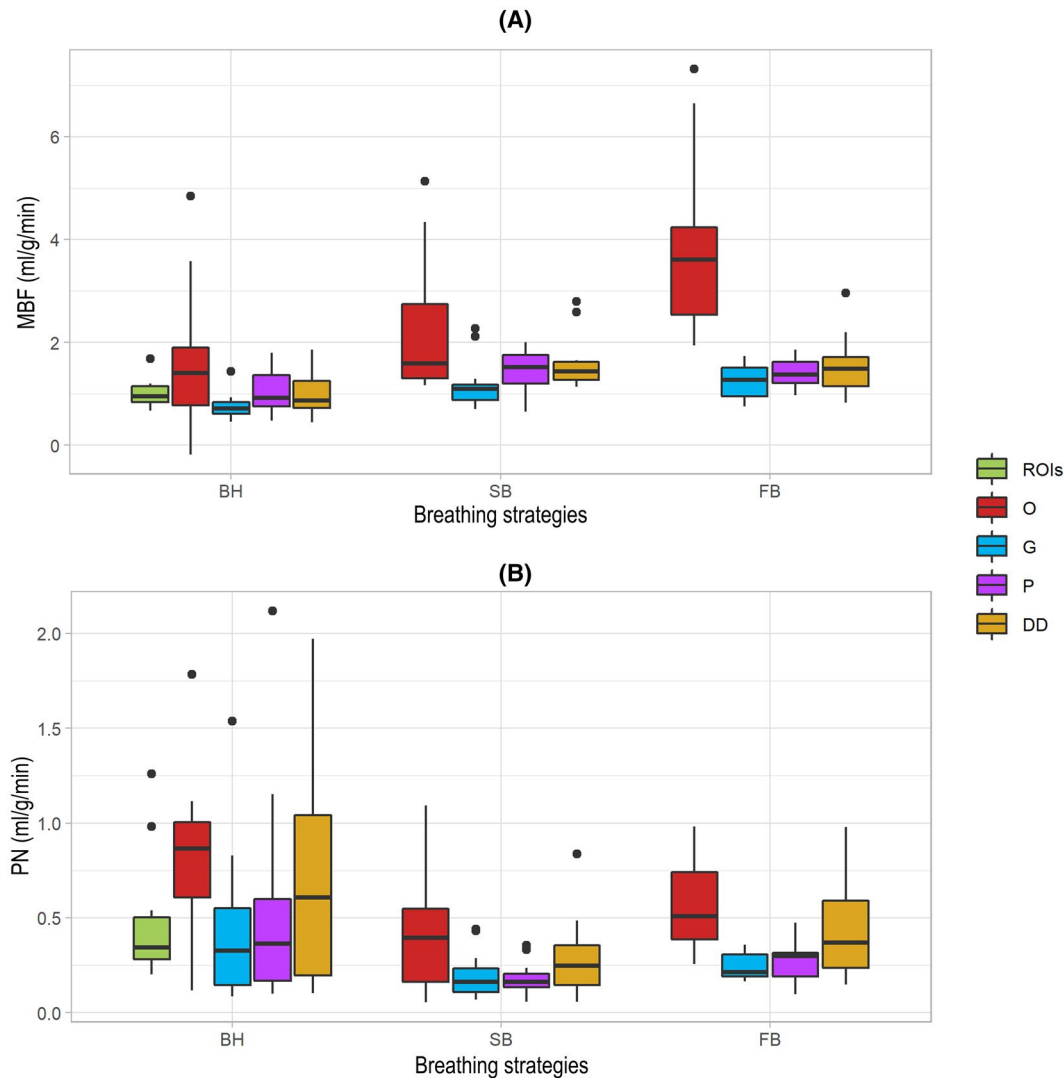
FIGURE 4 Motion evaluation in in vivo images. Boxplots for: (A) MBF and (B) PN measurements in units of ml/g/min. Data from the first ASL acquisition was considered. The black line within the box indicates the median value. Boxes represent the interquartile range (25%-75%). The whiskers extend to the most extreme data points not considered outliers. Outliers are represented as black dots. ROIs (in green), O (in red), G (in blue), P (in pink), and DD (in orange). For significant *P* values, see Table 3. DD, after detecting and discarding motion outliers; G, after groupwise registration; MBF, myocardial blood flow; O, without motion correction; P, after pairwise registration; PN, physiological noise; ROI, region of interest; ROIs, 1 ROI per perfusion-weighted image

subjects to hold their breath following these instructions. The effect of motion between breath-holds was minimized by manually delineating the myocardium in each PWI. This strategy was designed as reported by previous myocardial ASL studies,[5–8] with shorter acquisition time than SB and FB scans. An acquisition time of 5 min was not considered feasible in this case because it would have required the performance of 15 breath-holds to complete the study, which can be demanding, especially in patient populations. Instead, the acquisition was reduced to 12 images, expanding 2 min approximately. The obtained reference perfusion measurements analyzed with individual ROIs per PWI were in line with those reported in the literature for healthy subjects.[29]

The SB strategy involved the subject's coordination of the respiration with the TR of the sequence. It was a more time-efficient strategy than BH for the acquisition of a larger set of images due to the fact that no breath-holding instructions were required, which saved time between acquisitions. In this work, we showed that its application was feasible in myocardial ASL but that data quality was dependent on the subject's performance, which improved with repetition and required the use of motion-correction techniques.

The FB strategy did not require collaboration during data acquisition, but motion correction played a fundamental role. In fact, both synthetic and in vivo original perfusion measurements were significantly overestimated

TABLE 3 *P* values obtained in the post hoc comparisons of the nonparametric factorial ANOVA to evaluate in vivo differences in MBF and PN across 2 factors: breathing strategy (3 levels = BH, SB, and FB) and motion correction technique (4 levels = O, G, P, and DD)

Motion correction	*P* values		Breathing strategies	*P* values	
	PN	MBF		PN	MBF
DD – G	0.0014	0.0035	BH – FB	0.0208	< 0.0001
DD – O	NS	< 0.0001	BH – SB	< 0.0001	0.0001
DD – P	0.0178	NS	SB – SB	0.0009	0.0018
G – O	< 0.0001	< 0.0001			
G – P	NS	0.0149			
O – P	< 0.0001	< 0.0001			

P values are adjusted for Bonferroni correction.

Abbreviations: ANOVA, analysis of variance; BH, breath-hold; DD, after detecting and discarding motion outliers; FB, free-breathing; G, after groupwise registration; MBF, myocardial blood flow; NS, nonsignificant; O, without motion correction; P, after pairwise registration; PN, physiological noise; SB, synchronized-breathing.

TABLE 4 In vivo measurements obtained from the different ASL datasets for all breathing strategies and motion correction techniques

		MBF (ml/g/min)		PN (ml/g/min)		CV$_{MBF}$ (%)		wsCV (%)
		Acq 1	Acq 2	Acq 1	Acq 2	Acq 1	Acq 2	
BH	ROIs	1.00 ± 0.28	1.09 ± 0.25	0.48 ± 0.32	0.26 ± 0.24	28	23	16
	O	1.68 ± 1.40	1.65 ± 1.10	0.81 ± 0.45	0.79 ± 0.61	83	67	32
	DD	1.03 ± 0.52	1.10 ± 0.26	0.68 ± 0.57	0.55 ± 0.51	50	23	29
	G	0.75 ± 0.26	0.88 ± 0.22	0.45 ± 0.42	0.36 ± 0.34	35	25	24
	P	1.03 ± 0.42	1.00 ± 0.43	0.56 ± 0.59	0.42 ± 0.36	41	42	22
SB	O	2.29 ± 1.38	1.70 ± 0.69	0.40 ± 0.31	0.20 ± 0.11	60	40	45
	DD	1.61 ± 0.54	1.46 ± 0.22	0.29 ± 0.22	0.22 ± 0.09	33	15	22
	G	1.18 ± 0.51	1.20 ± 0.42	0.20 ± 0.13	0.18 ± 0.09	43	35	20
	P	1.42 ± 0.43	1.31 ± 0.30	0.18 ± 0.12	0.19 ± 0.10	30	23	17
FB	O	3.79 ± 1.72	3.60 ± 1.03	0.57 ± 0.25	0.55 ± 0.25	45	29	27
	DD	1.55 ± 0.58	1.66 ± 0.45	0.43 ± 0.25	0.41 ± 0.23	37	27	20
	G	1.25 ± 0.35	1.30 ± 0.40	0.24 ± 0.07	0.29 ± 0.16	28	31	15
	P	1.39 ± 0.29	1.34 ± 0.28	0.26 ± 0.11	0.31 ± 0.21	21	21	11

MBF and PN in units of mL/g/min are reported as mean ± SD across subjects. CV$_{MBF}$ and wsCV are reported in percentage (%). PB was computed as the ratio of the MBF SD to the square root of the number of perfusion-weighted images. CV$_{MBF}$ was computed as the ratio of the MBF group SD to the group mean.

Abbreviations: Acq$_1$, first ASL acquisition; Acq$_2$, second ASL acquisition; CV$_{MBF}$, coefficient of variation of MBF; DD, after detecting and discarding motion outliers; G, after groupwise registration; MBF, myocardial blood flow; O, without motion correction; P, after pairwise registration; PN, physiological noise; ROI, region of interest; ROIs, 1 ROI per perfusion-weighted image; wsCV, within-subject coefficient of variation.

(Figures 2 and 4), likely due to contamination of the perfusion measurement with the blood pool signal in the presence of motion. In synthetic data, the original measurements were much larger than the reference values, resulting in large accuracy errors. The use of registration minimized this effect. The performance of both pairwise and groupwise registration approaches was satisfactory in vivo, where perfusion after pairwise registration showed a slightly lower variability across subjects and higher reproducibility. In synthetic data, perfusion measurements after pairwise registration showed lower accuracy errors. When motion was introduced, accuracy error was also lower after the pairwise approach regardless of the applied transformation and amplitude, showing its capability to

correct for both minor and extreme motion. Overall, these findings suggest a superior performance of the pairwise over the groupwise registration approach.

There are several possible explanations for this result. The pairwise approach registers all images by repeatedly optimizing the transformation of each pair independently. On the contrary, the groupwise approach registers all images in a single optimization. This is achieved by creating a common space from the entire dataset represented by the K correlation matrix from which the principal components are obtained. Simultaneously registering the 63 images acquired in 1 ASL dataset, including the baseline image, involves the use of a complex model with more degrees of freedom in comparison to the pairwise
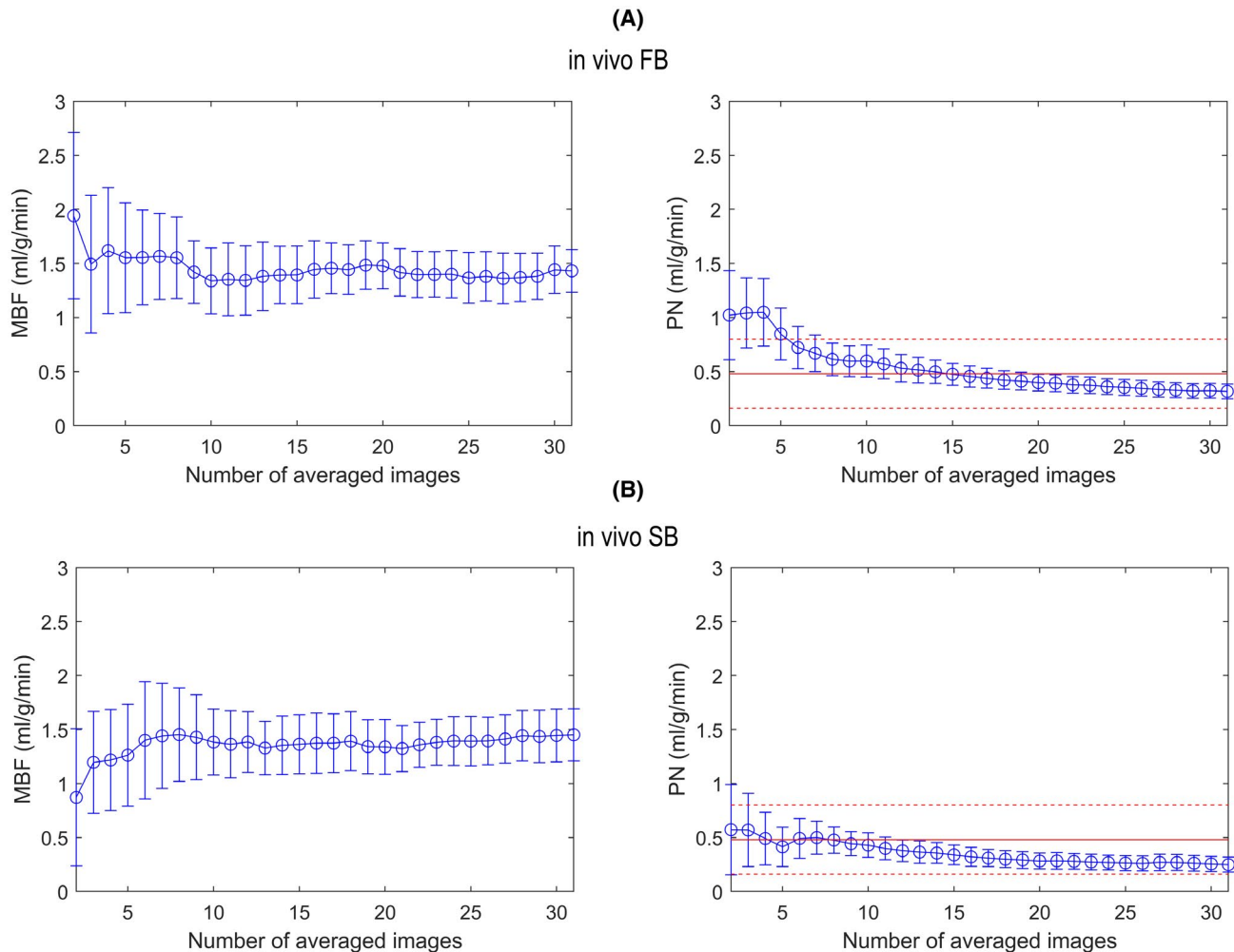
(A)

in vivo FB

(B)

in vivo SB

FIGURE 5 MBF and PN computed after pairwise registration of the first acquisition as a function of the number of averages. (A) In vivo FB dataset. (B) In vivo SB dataset. In all graphs, group means are depicted. Error bars represent the SD across subjects. In the PN graphs, red lines indicate the PN computed in the reference breath-holding dataset (analyzed with 1 myocardial region of interest per perfusion-weighted image). Continuous line indicates the mean and discontinuous lines represent the group SD. FB, free-breathing; MBF, myocardial blood flow; PN, physiological noise; SB, synchronized-breathing

registration. Therefore, there is a greater chance of model overfitting. The performance of this method could be potentially improved by regularizing the described PCA metric; however, this needs to be tested in this particular application. In addition, the intensity contrast differences between label and control images (where there is a strong alternating signal of the ventricular blood pool) might also contribute to the differences found in the performance of both registration methods. In the pairwise approach, 1 single label-control registration is carried out; subsequently, label and control images are registered to their corresponding reference images, which have similar intensities. However, in the groupwise approach, the simultaneous registration of all images with different intensities could add more complexity and affect the performance of the method.

Groupwise registration approaches have been successfully used in renal ASL[30,31]; however, intensity differences between label and control kidney images are small. In the context of cardiac images, groupwise registration has also been applied to T1 mapping[21] or first-pass perfusion[32] datasets, but again the intensity change across images is lower than that encountered in myocardial FAIR ASL. Future work could explore the use and performance of other groupwise metrics in the context of myocardial ASL, such as the sum of variances,[33] total correlation,[34] or conditional template entropy.[35]

The evaluation of the number of PWIs required to match the PN performance of the reference BH dataset showed that it is necessary to average 15 and 8 PWIs for FB and SB strategies, respectively. For a higher number of averages, the PN continued to decrease, but the benefit of
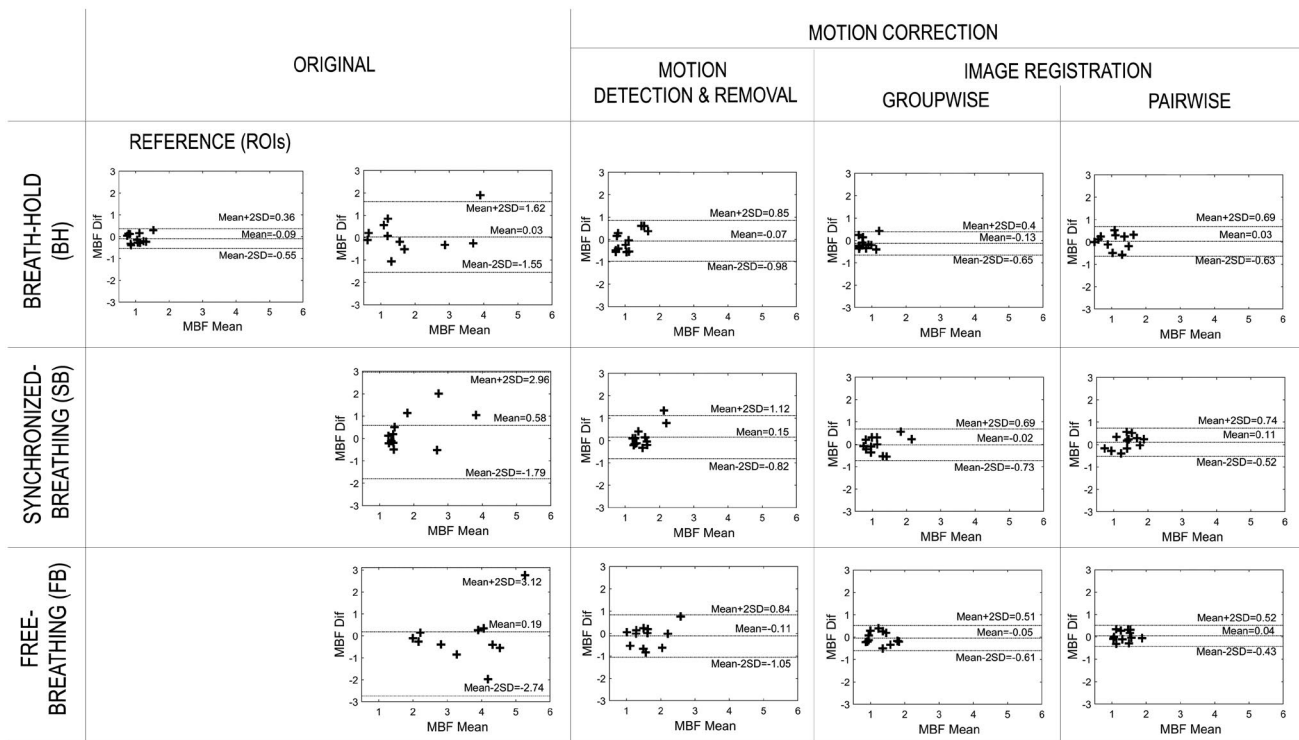
FIGURE 6 Bland-Altman plots comparing in vivo MBF intrasession measurements in units of ml/g/min for all perfusion datasets. The original breath-holding dataset was analyzed using both a single ROI drawn over the mean perfusion-weighted image and 1 ROI drawn over each perfusion-weighted image (ROIs). The latter was considered as reference in in vivo data. MBF, myocardial blood flow; ROI, region of interest

averaging was reduced. This result could be used to optimize the acquisition time in forthcoming studies.

The procedure to detect and discard motion outliers was also satisfactory, showing improved reproducibility and lower variability across subjects than original datasets. This suggests a better detection of motion-corrupted images acquired at inspiration, in comparison to the application of the "mean ± 2SD" criterion to the PWIs, for the identification of extreme outliers. The number of outliers detected with this approach was similar to those reported by Capron et al.,[36] with a retrospective image exclusion algorithm based on the cross-correlation of myocardial contours. Perfusion measurements obtained after rejecting outliers were significantly different from those obtained without registration and after groupwise registration.

Intrasession reproducibility of the perfusion measurements evaluated through the wsCV after motion correction ranged from 11% to 29%. These values were comparable to previous ASL studies that reported a 17% for FB datasets combined with registration,[16] a 21.8% for navigator-gating acquisitions in combination with nonrigid registration,[15] and a 13% for BH acquisitions using a Look-Locker FAIR ASL sequence.[13]

This study has several limitations. The number of images acquired in BH was lower than those acquired in SB and FB datasets, which likely had an effect in

the BH results. However, as previously mentioned, an increased number of breath-holds is difficult to realize in practice and will be especially challenging in patient populations. It thus was not attempted in this study. It might be interesting to compare the results of this study with those obtained from the automatic segmentation of the myocardium, which has been tested in the context of cardiac ASL with deep convolutional neural networks.[37] The respiratory synchronization was dependent on the patient's performance. Future investigations might achieve better synchronization by directly guiding on the appropriate timing to perform each breath-hold. The performance of the breathing strategies was only tested in rest studies. Forthcoming studies could compare their application under stress conditions to increase the perfusion signal and evaluate their effects in higher SNR measurements.

5 | CONCLUSION

The results of this work demonstrated that both SB and FB ASL strategies were able to provide accurate perfusion measurements after motion correction, which effectively minimized MBF overestimation caused by motion in the original datasets. In addition, this study determined the number of

PWIs needed in each strategy (8 in SB; 15 in FB) to match the performance of the BH acquisition with 6 PWIs.

In particular, synthetic and experimental results agreed on the superiority of FB after pairwise registration, which showed higher accuracy and robustness to motion in synthetic images and higher intrasession reproducibility together with lower MBF variability across subjects in in vivo images. The series of BH and SB after motion correction provided similar results; however, these breathing techniques can be difficult to perform, especially by patients with suspected coronary artery disease due to associated comorbidities such as heart failure that can lead to chronic obstructive pulmonary disease.

CONFLICT OF INTEREST
Marta Vidorreta is an employee of Siemens Healthineers in Spain. The authors have no other conflicts of interest to declare.

ORCID
Verónica Aramendía-Vidaurreta https://orcid.org/0000-0001-9834-2866
Pedro M. Gordaliza https://orcid.org/0000-0001-5305-3104
Rebeca Echeverría-Chasco https://orcid.org/0000-0003-0199-2593
Arrate Muñoz-Barrutia https://orcid.org/0000-0002-1573-1661
María A. Fernández-Seara https://orcid.org/0000-0001-8536-6295

REFERENCES
1. Virani SS, Alonso A, Benjamin EJ, et al. Heart disease and stroke statistics-2020 update: a report from the American Heart Association. *Circulation*. 2020;141:e139-e596.
2. Global Burden of Disease Collaborative Network. *Global Burden of Disease Study 2017 (GBD 2017)*. Institute for Health Metrics and Evaluation. Available at: https://ourworldindata.org/causes-of-death#what-do-people-die-from. 2018.
3. Detre JA, Leigh JS, Williams DS, Koretsky AP. Perfusion imaging. *Magn Reson Med*. 1992;23:37-45.
4. Kober F, Jao T, Troalen T, Nayak KS. Myocardial arterial spin labeling. *J Cardiovasc Magn Reson*. 2016;18:22.
5. Zun Z, Wong EC, Nayak KS. Assessment of myocardial blood flow (MBF) in humans using arterial spin labeling (ASL): feasibility and noise analysis. *Magn Reson Med*. 2009;62:975-983.
6. Zun Z, Varadarajan P, Pai RG, Wong EC, Nayak KS. Arterial spin labeled CMR detects clinically relevant increase in myocardial blood flow with vasodilation. *JACC Cardiovasc Imaging*. 2011;4:1253-1261.
7. Do HP, Jao TR, Nayak KS. Myocardial arterial spin labeling perfusion imaging with improved sensitivity. *J Cardiovasc Magn Reson*. 2014;16:15.
8. Yoon AJ, Do HP, Cen S, et al. Assessment of segmental myocardial blood flow and myocardial perfusion reserve by adenosine-stress myocardial arterial spin labeling perfusion imaging. *J Magn Reson Imaging*. 2017;46:413-420.
9. Poncelet BP, Koelling TM, Schmidt CJ, et al. Measurement of human myocardial perfusion by double-gated flow alternating inversion recovery EPI. *Magn Reson Med*. 1999;41:510-519.
10. Do HP, Yoon AJ, Fong MW, Saremi F, Barr ML, Nayak KS. Double-gated myocardial ASL perfusion imaging is robust to heart rate variation. *Magn Reson Med*. 2016;77:1975-1980.
11. Lapi S, Lavorini F, Borgioli G, et al. Respiratory rate assessments using a dual-accelerometer device. *Respir Physiol Neurobiol*. 2014;191:60-66.
12. Wang Y, Riederer SJ, Ehman RL. Respiratory motion of the heart: kinematics and the implications for the spatial resolution in coronary imaging. *Magn Reson Med*. 1995;33:713-719.
13. Keith GA, Rodgers CT, Chappell MA, Robson MD. A look-locker acquisition scheme for quantitative myocardial perfusion imaging with FAIR arterial spin labeling in humans at 3 Tesla. *Magn Reson Med*. 2017;78:541-549.
14. Aramendía-Vidaurreta V, Echeverría-Chasco R, Vidorreta M, Bastarrika G, Fernández-Seara MA. Quantification of myocardial perfusion with vasodilation using arterial spin labeling at 1.5T. *J Magn Reson Imaging*. 2021;53:777-788.
15. Wang DJJ, Bi X, Avants BB, Meng T, Zuehlsdorff S, Detre JA. Estimation of perfusion and arterial transit time in myocardium using free-breathing myocardial arterial spin labeling with navigator-echo. *Magn Reson Med*. 2010;64:1289-1295.
16. Aramendía-Vidaurreta V, García-Osés A, Vidorreta M, Bastarrika G, Fernández-Seara MA. Optimal repetition time for free breathing myocardial arterial spin labeling. *NMR Biomed*. 2019;32:e4077.
17. Robson PM, Madhuranthakam AJ, Dai W, Pedrosa I, Rofsky NM, Alsop DC. Strategies for reducing respiratory motion artifacts in renal perfusion imaging with arterial spin labeling. *Magn Reson Med*. 2009;61:1374-1387.
18. Makela T, Clarysse P, Sipila O, et al. A review of cardiac image registration methods. *IEEE Trans Med Imaging*. 2002;21:1011-1021.
19. Javed A, Jao TR, Nayak KS. Motion correction facilitates the automation of cardiac ASL perfusion imaging. *J Cardiovasc Magn Reson*. 2015;17:P51.
20. Avants BB, Epstein CL, Grossman M, Gee JC. Symmetric diffeomorphic image registration with cross-correlation: evaluating automated labeling of elderly and neurodegenerative brain. *Med Image Anal*. 2008;31:1713-1723.
21. Huizinga W, Poot D, Guyader J-M, et al. PCA-based groupwise image registration for quantitative MRI. *Med Image Anal*. 2016;29:65-78.
22. Klein S, Staring M, Murphy K, Viergever MA, Pluim JPW. Elastix: a toolbox for intensity-based medical image registration. *IEEE Trans Med Imaging*. 2010;29:196-205.
23. *Elastix Parameter File Database Webpage*. Available at: https://elastix.lumc.nl/modelzoo/par0039/ Accessed September 2021.
24. Lu H, Clingman C, Golay X, Van Zijl PCM. Determining the longitudinal relaxation time (T1) of blood at 3.0 Tesla. *Magn Reson Med*. 2004;52:679-682.

25. Wobbrock JO, Findlater L, Darren Gergle JJH. The aligned rank transform for nonparametric factorial analyses using only ANOVA procedures. In Proceedings CHI 2011: the 29th Annual CHI Conference on Human Factors in Computing Systems, Vancouver, BC, Canada, 2011. p. 143-146.

26. Jones R, Payne B. *Clinical Investigation and Statistics in Laboratory Medicine*. ACB Venture Publications; 1997.

27. Software MedCalc. *Coefficient of Variation from Duplicate Measurements*. ACB Venture Publications. Available at: https://www.medcalc.org/manual/cvfromduplicates.php. Accessed May 10, 2021.

28. Epstein FH, Meyer CH. Myocardial perfusion using arterial spin labeling CMR: promise and challenges. *JACC Cardiovasc Imaging*. 2011;4:1262-1264.

29. Chareonthaitawee P. Heterogeneity of resting and hyperemic myocardial blood flow in healthy humans. *Cardiovasc Res*. 2001;50:151-161.

30. Echeverria-Chasco R, Vidorreta M, Aramendía-Vidaurreta V, et al. Optimization of pseudo-continuous arterial spin labeling for renal perfusion imaging. *Magn Reson Med*. 2021;85:1507-1521.

31. Harteveld AA, de Boer A, Franklin SL, Leiner T, van Stralen M, Bos C. Comparison of multi-delay FAIR and pCASL labeling approaches for renal perfusion quantification at 3T MRI. *MAGMA*. 2020;33:81-94.

32. Mahapatra D. Joint segmentation and groupwise registration of cardiac perfusion images using temporal information. *J Digit Imaging*. 2013;26:173-182.

33. Metz CT, Klein S, Schaap M, van Walsum T, Niessen WJ. Nonrigid registration of dynamic medical imaging data using nD+t B-splines and a groupwise optimization approach. *Med Image Anal*. 2011;15:238-249.

34. Guyader JM, Huizinga W, Fortunati V, et al. Total correlation-based groupwise image registration for quantitative MRI. In Proceedings of the 29th IEEE Conference on Computer Vision and Pattern Recognition Workshops, Las Vegas, 2016. p. 626-633.

35. Polfliet M, Klein S, Huizinga W, Paulides MM, Niessen WJ, Vandemeulebroucke J. Intrasubject multimodal groupwise registration with the conditional template entropy. *Med Image Anal*. 2018;46:15-25.

36. Capron T, Troalen T, Robert B, Jacquier A, Bernard M, Kober F. Myocardial perfusion assessment in humans using steady-pulsed arterial spin labeling. *Magn Reson Med*. 2015;74:990-998.

37. Do HP, Guo Y, Yoon AJ, Nayak KS. Accuracy, uncertainty, and adaptability of automatic myocardial ASL segmentation using deep CNN. *Magn Reson Med*. 2020;83:1863-1874.

SUPPORTING INFORMATION

Additional supporting information may be found in the online version of the article at the publisher's website.

FIGURE S1 Respiratory motion detection procedure. (A) Top images show the respiratory movement of the diaphragm. During expiration (left), air gets out of the lungs and the diaphragm relaxes and moves up. During inspiration (right), air gets into the lungs and the diaphragm contracts and descends. Bottom images show the position of the heart both at expiration and inspiration. The x symbol represents the selected voxel in the anterior myocardial segment. (B) Short-axis images of the heart from a representative volunteer. On the left, an image acquired during expiration. On the right, an image acquired during inspiration. In the middle, signal intensity across the superior to inferior (S-I) direction and along the temporal series of images. The blue arrow points to a representative image acquired during inspiration containing gray signal from the myocardium at the selected voxel. The red arrow points to a representative image acquired during expiration containing black signal from the lungs at the selected voxel

FIGURE S2 Set of transformations applied to synthetic data considering a five-amplitude range. (A) Synthetic control images, (B) Synthetic label images. Translation corresponds to the horizontal and vertical displacement of the image measured in pixels. Rotation corresponds to the rotation of the myocardium around the center point of the image measured in degrees. Shear corresponds to the horizontal shear of the image measured in degrees

FIGURE S3 Procedure to automatically select the reference image in a pairwise registration. (A) edges obtained after the application of the Canny edge filter; (B) ROI defined covering the myocardium over the average edge image; (C) ROI defined covering the left-ventricular blood pool over the average edge image; (D) ROI covering the myocardium; (E) edges within the ROI myocardial mask created in step D; (F) cross-correlation between label and control edge images for the selection of the highest correlated image pair (represented as a green point). ROI, region of interest

TABLE S1 Motion detection in all breathing strategies: The number of perfusion-weighted images (PWIs) used to analyse datasets after motion detection is reported as the number of discarded and remaining PWIs per subject